EUROPEAN CONFERENCE ON INTEGRATED OPTICS

Third-Order Intermodulation Distortion Suppression Analysis for Dual-Parallel Mach-Zehnder Modulator Using Optical Carrier Band Processing

Cristina Catalá-Lahoz[1], Luis Torrijos-Morán[1], Daniel Pérez-López[2], Li Xu[3], Wang Tianxiang[3] and Diego Pérez-Galacho[1*]

[1]Photonics Research Labs, iTEAM Research Institute, Universitat Politècnica de València, Valencia, 46022, Spain
[2]iPronics Programmable Photonics S.L., Av. de Blasco Ibáñez, 25, Valencia, 46010, Spain
[3]Central Research Institute, Huawei Co. LTD.
[*]diepega@upv.es

Third-order distortion in microwave photonic links using dual-parallel Mach-Zehnder modulators is theoretically studied for linearization. Four-tone test is considered in the mathematical derivation and results show that linearization is feasible under a proper tuning of DC operation voltages of the modulator and processing of the optical spectrum. Simulations are also provided showing a 34 dBm suppression at the third-order intermodulation products.
Keywords: *Electro-optic modulators, Linearization, Microwave Photonics, Optics.*

INTRODUCTION

Microwave photonic links (MPL) offer several advantages compared to conventional electrical schemes such as broadband operation, lightweight, immunity to electromagnetic interference and low loss. This fact makes them an interesting option for different radio frequency (RF) applications as in the case of antenna remoting, radio-over-fiber, or wireless communications, among others [1]. In this context, the main limitation factor of MPL usually comes from the electro-optic modulator that introduces nonlinearity in the rest of the link. Third-order intermodulation distortion (IMD3) is the most challenging nonlinearity produced as it lies close to the fundamental tones and cannot be easily filtered [2]. To improve the linearity of modulators in MPL, the modulated optical spectrum is processed to compensate the distortion terms produced by the beating at the PD [3],[4]. The linearization of more complex modulation schemes based on dual-parallel MZM (DPMZM) was also investigated by adjusting the power of the electrical drive signals, the optical input power splitting ratios, optimizing the operation points in single-drive configurations or shifting the electrical phase of the RF inputs [5]–[8]. To date, all these DPMZM linearization approaches are based either on RF predistortion techniques or using one of the parallel MZM to improve the linearity of the complete structure. An exhaustive mathematical description of the DPMZM linearization is still to be investigated. In this paper, we show a complete analysis of the distortion appearing in DPMZM when two RF signals (each one containing two different tones) are applied in both the upper and lower MZM of the DPMZM, so that a four-tone test is considered. Theoretical results and simulations are provided, describing the cancelation of all the IMD3 components that are produced at the PD.

RESULTS

The proposed MPL is depicted in Fig. 1a. It consists of a DPMZM in push-pull configuration (that is a phase shift of π between driving RF signals at each MZM arm). As it is shown, the optical carrier is therefore modulated by two different RF signals: RF_1 ($\omega_{1,2}$) and RF_2 ($\omega_{3,4}$) for the lower and upper MZM, respectively, so that we consider a four-tone test.

The field after modulation can be expressed as follows

$$E_{out}(t) \propto e^{j\phi_3}\left[e^{j\phi_1}S_1(m) + S_1(-m)\right] + \left[e^{j\phi_2}S_2(m) + S_2(-m)\right]. \quad (1)$$

Where $S_{1,2}(m)$ expressions correspond to each individual MZM and are defined in terms of Bessel functions as

$$S_1(m) = \sum_{n=-\infty}^{+\infty} J_n(m)e^{jn\omega_1 t} \sum_{k=-\infty}^{+\infty} J_k(m)e^{jk\omega_2 t}, \quad (2)$$

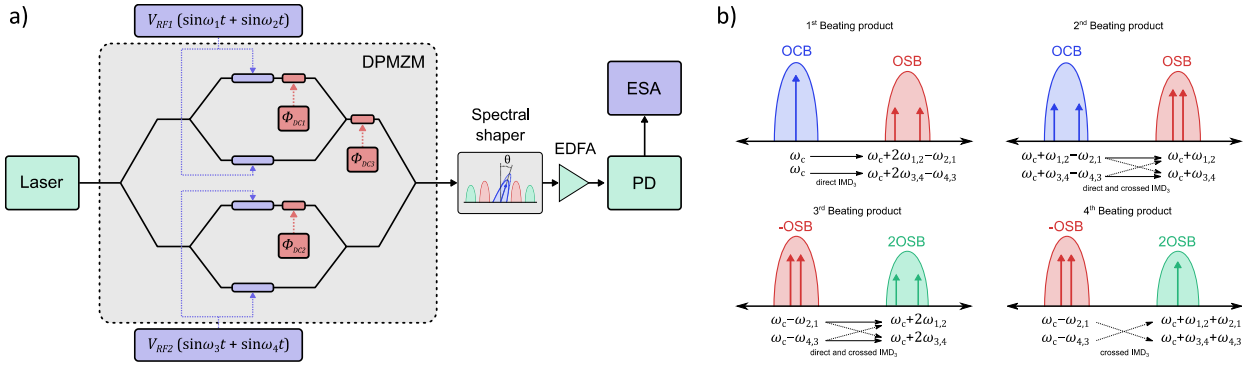

Fig. 1. a) MPL considered including the DPMZM under a four-tone test, the laser, optical processor for the linearization, erbium-doped fiber amplifier (EDFA), photodetector (PD) and electronic spectrum analyzer (ESA). b) Representation of the optical modulated spectrum and the different beating products that produce IMD3.

$$S_2(m) = \sum_{n=-\infty}^{+\infty} J_n(m) e^{jn\omega_3 t} \sum_{k=-\infty}^{+\infty} J_k(m) e^{jk\omega_4 t}. \tag{3}$$

Up to four beating products (BPs) are obtained, producing IMD$_3$ at the photodiode, see Fig. 1b. The first one produces direct IMD$_3$ terms (that only depend on one of the RF frequencies, —e.g., $2\omega_1 - \omega_2$). The second BP in turn produces direct IMD$_3$ terms and crossed IMD$_3$ terms that depend on both RF$_1$ ($\omega_{1,2}$) and RF$_2$ ($\omega_{3,4}$) frequencies —e.g., $\omega_1 - \omega_2 + \omega_3$. The third BP involves both direct and crossed IMD$_3$ terms —e.g., $2\omega_1 - \omega_2$ and $2\omega_1 - \omega_3$. Finally, the fourth BP produces only crossed terms —e.g., $\omega_1 + \omega_2 - \omega_3$. After PD, we can classify the 8 contributors for IMD$_3$ terms depending on the BP that produce them as follows

$$\begin{aligned} I_{PD} = R_{PD}|E_p|^2 = {} & I_{3,1}\sin\left((2\omega_{1,2} - \omega_{2,1})t\right) + I_{3,2}\sin\left((2\omega_{3,4} - \omega_{4,3})t\right) + \\ & I_{3,3}\sin\left((2\omega_{1,1,2,2} - \omega_{3,4,3,4})t\right) + I_{3,4}\sin\left((2\omega_{3,3,4,4} - \omega_{1,2,1,2})t\right) + \\ & I_{3,5}\sin\left((\omega_{3,3,4,4} - \omega_{4,4,3,3} + \omega_{1,2,1,2})t\right) + I_{3,6}\sin\left((\omega_{1,1,2,2} - \omega_{2,2,1,1} + \omega_{3,4,3,4})t\right) + \\ & I_{3,7}\sin\left((\omega_{1,1} + \omega_{2,2} - \omega_{3,4})t\right) + I_{3,8}\sin\left((\omega_{3,3} + \omega_{4,4} - \omega_{1,2})t\right), \end{aligned} \tag{4}$$

where R_{PD} is the responsivity of the PD, $I_{3,1}$, $I_{3,2}$ are direct IMD$_3$, and $I_{3,3}$, $I_{3,4}$, $I_{3,5}$, $I_{3,6}$, $I_{3,7}$ and $I_{3,8}$ are crossed IMD$_3$ terms, previously explained.

By multiplying Eq. (1) by its conjugate we obtain the current at the PD so that we can relate it to all I_3 terms using Eq. (4). For the first and second direct IMD$_3$ coefficient $I_{3,1}$ and $I_{3,2}$, these yields

$$I_{3,1} = 4R_{PD}P_i(k - k^2) \cdot \left[\frac{1}{2}\beta\sin\phi_1 + \Phi_1 A J_0^2 J_1 J_2\right] \tag{5}$$

$$I_{3,2} = 4R_{PD}P_i(k - k^2) \cdot \left[\frac{1}{2}\beta\sin\phi_2 - \Phi_2 A J_0^2 J_1 J_2\right] \tag{6}$$

whence β, Φ_1 and Φ_2 are defined as

$$\beta = A J_0^2 J_1 J_2 \cos\theta + A J_0 J_1^3 \cos\theta + J_0^2 J_1 J_2, \tag{7}$$

$$\Phi_1 = \sin(\phi_1 - \phi_2 + \phi_3 - \theta) + \sin(\phi_1 + \phi_3 - \theta) - \sin(-\phi_2 + \phi_3 - \theta) - \sin(\phi_3 - \theta), \tag{8}$$

$$\Phi_2 = \sin(\phi_1 - \phi_2 + \phi_3 - \theta) - \sin(\phi_1 + \phi_3 + \theta) + \sin(-\phi_2 + \phi_3 + \theta) - \sin(\phi_3 + \theta). \tag{9}$$

where A and θ is the amplitude suppression and phase shift imposed to the OCB by the spectral shaper, respectively. On the other hand, assuming $\phi_1 = -\phi_2$ and no OCB processing —i.e., $A = 1$ and $\theta = 0$, all crossed

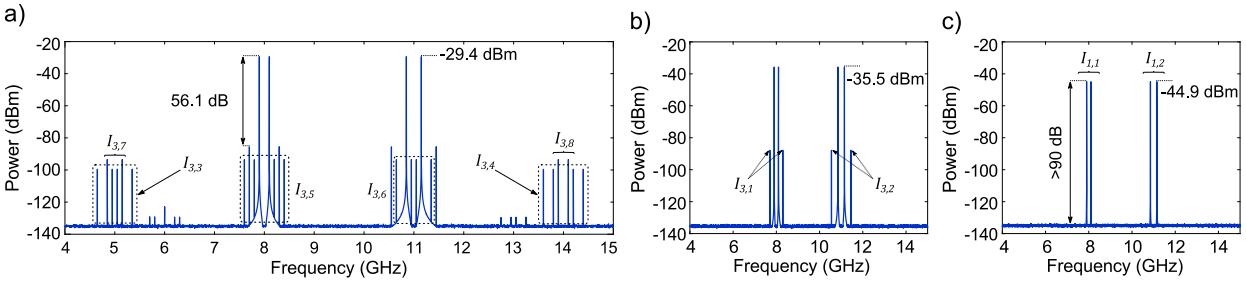

Fig. 2. a) Simulated MPL RF spectrum without linearization tuning. b) RF spectrum with the cancelation of crossed IMD₃ terms . c) RF spectrum of the complete linearization configuration including OCB processing.

IMD₃ terms ($I_{3,3}, I_{3,4}, I_{3,5}, I_{3,6}, I_{3,7}, I_{3,8}$) are directly proportional to the phase shifts applied by the DC voltages, and can be described by the following expression

$$I_{3,C} \propto \sin(2\phi_1 + \phi_3) - \sin(\phi_3). \tag{10}$$

To cancel crossed IMD₃ terms, we must first equal Eq. (8) to zero. Fixing $\phi_3 = 2\phi_1$ the equation is solved for $\phi_3 = \pi$, thus $\phi_1 = \pi/2$ and $\phi_2 = -\pi/2$. Now, to calculate θ, we introduce these values in Φ_1 and Φ_2 expressions and solve the system of equations, which yields $\theta = \pi$. Finally, to fully cancel direct IMD₃ terms, we solve β in Eq. (7) for this value of θ applying Taylor series expansion to the third order in m (small signal approximation). This condition if fulfilled when an amplitude suppression of $A = 1/3$ is applied to the OCB, so that direct IMD₃ contributors in Eq. (5) and (6) are theoretically canceled. Figure 2a shows the simulated RF spectrum without linearization, —i.e., the bias voltages of the DPMZM $\phi_1 = \phi_2 = \pi/2$, $\phi_3 = 0$ and no OCB processing, $\theta = 0$ and $A = 1$. The resulting RF spectrum contains all the IMD₃ theoretically described including both direct and crossed terms. A fundamental to IMD₃ ratio (FIR) of 56.1 dBm is obtained at this stage. Figure 2b contains the RF spectrum with only the DC bias voltages adjusted to suppress IMD₃ crossed terms in Eq. (8), —i.e., $\phi_1 = \pi/2, \phi_2 = -\pi/2, \phi_3 = \pi$ and no OCB processing. Only direct IMD₃ are obtained in the spectrum. Figure 2c depicts the linearized RF spectrum with the theoretical values obtained before: $\phi_1 = \frac{\pi}{2}, \phi_2 = -\frac{\pi}{2}, \phi_3 = \pi$, an attenuation of $A = 1/3$ and phase of $\theta = \pi$ imposed on the OCB. Simulations show a FIR over 90 dBm, which means an IMD₃ suppression above 33.9 dBm compared to Fig. 2a.

DISCUSSION

In conclusion, OCB processing to linearize a MPL based on a DPMZM is theoretically demonstrated. A four-tone test is considered in the study, which allow us to provide an exhaustive mathematical derivation of all IMD3 terms that are produced in the PD mixing. Simulations show that crossed IMD3 terms can be cancelled out by properly tuning the DC voltages of the modulator, while direct IMD3 terms need from a precise OCB processing to completely linearize the link. Overall, the theoretical description herein presented extends mathematical derivations in previous works to a more complete structure, enabling the modulation of two different RF signals simultaneously, up to 4 frequencies, with complete isolation and no distortion between them. Moreover, the linearization method does not need any extra RF components and other predistortion devices, which allows its integration and development in integrated circuits.

References

[1] J. Capmany and D. Novak, "Microwave photonics combines two worlds," Nat. Photonics **1**, 319–330 (2007).
[2] J. Yao, "Microwave photonics," J. Light. Technol. 27, 314–335 (2009).
[3] Y. Cui, Y. Dai, F. Yin, J. Dai, K. Xu, J. Li and J. Lin, "Intermodulation distortion suppression for intensity-modulated analog fiber-optic link incorporating optical carrier band processing," Opt. Express 21, 23433 (2013).
[4] G. Liu, O. Daulay, Q. Tan, H. Yu and D. Marpaung "Linearized phase modulated microwave photonic link based on integrated ring resonators," Opt. Express 28, 38603 (2020).
[5] Y. Zhou, L. Zhou, M. Wang, Y. Xia, Y. Zhong, X. Li and J. Chen "Linearity characterization of a dual-parallel silicon Mach-Zehnder modulator," IEEE Photonics J. 8, (2016).
[6] S. Kim, W. Liu, Q. Pei, L. R. Dalton and H.R. Fetterman "Nonlinear intermodulation distortion suppression in coherent analog fiber optic link using electro-optic polymeric dual parallel Mach-Zehnder modulator," Opt. Express 19, 7865-7871 (2011).
[7] S. Li, X. Zheng, H. Zhang and B. Zhou "Highly Linear Radio-Over-Fiber System Incorporating a Single-Drive Dual Parallel Mach-Zehnder Modulator," IEEE Photonics Technol. Lett 22, 1775-1777 (2010).
[8] W. Jiang, Q. Tan, W. Qin, D. Liang, X. Li, H. Ma and Z. Zhu "A linearization analog photonic link with high third-order intermodulation distortion suppression based on dual-parallel Mach-Zehnder modulator," IEEE Photonics J. 7, 2015).